IMPERFECT STOCHASTIC SYNCHRONIZATION OF THE NEAR WALL TURBULENCE

Sedat Tardu
Laboratoire des Ecoulements Géophysiques et Industriels
B.P. 53 X 38041 Grenoble, Cédex France
Sedat.Tardu@hmg.inpg.fr

Abstract

We investigate the characteristics of the instantaneous phases and amplitudes of the wavelet coefficients applied to the fluctuating wall shear stress and longitudinal velocity in the low buffer layer of a fully developed turbulent boundary layer. We show that the instantaneous phase exhibit long quiescent periods of constant values separated by sudden phase jumps. We establish a similarity with the stochastic synchronization of chaotic systems in the presence of noise that plays a role similar to the incoherent turbulence. We analyze the statistical characteristics of the constant phase periods and show the existence of type-I intermittency of the constant phase lengths related to a saddle-node bifurcation of the unstable periodic orbit embedded in the wall turbulent attractor. The period of the later is closely related to that of the cyclic regeneration of shear stress producing eddies.

Key words
Near wall turbulence, chaos synchronization, unstable periodic orbits, intermittency, coherent structures.

1 Introduction

The discovery of coherent structures in the early 1960's has profoundly modified our point of view of the wall turbulence structure. The pioneer work of Kline et al.[1], based on flow visualizations has revealed the existence of quasi-cyclic events, ordered in time and space, and largely contributing to the Reynolds shear stress production. Later, both experimental[2,3], and numerical[4] works have been devoted to the characterization of the wall coherent structures and several hundreds of papers related directly or indirectly to this topic have been published in the last four decades. The "incoherent" turbulence occupies only 20% of time and space in the inner layer. The coherent part is simpler to understand, since the coherent vortical structures can be identified, and tracked in time and space[5], and their direct effect on the wall shear and transport of the shear stresses and passive scalar can be clearly determined. The common consensus reached by now points at the existence of quasi-streamwise vortices of diameters typically 10 wall units and located at 20 units from the wall. Their streamwise extend is roughly 300 units, and they generate low and high speed streaks at the wall with a spanwise periodicity of 100 wall units. The sweep and ejection events they generate contribute to the Reynolds shear stress by 80%. The time period of their generation is approximately 100 units also and it depends on the distance from the wall [6,7].

Turbulence in general and the wall turbulence in particular can be seen as an infinite dimensional chaotic system. The quasi-periodicity induced by the coherent structures that are convecting in the low buffer layer, should logically lead to the synchronization of the turbulent quantities near the wall. Chaos synchronization is a process wherein chaotic coupled (sub)systems subject to external forcing adjust their time scales resulting in common spatial and temporal dynamics (Boccaletti et al.[8], Pikovsky et al[9]). Synchronization can also be defined as the locking between the instantaneous phases of a state variable of the system and the phase of the external periodic force. Several types of synchronization such as identical synchronization, phase synchronization, lag and generalized synchronization can be distinguished[10]. A rather weak degree of wall turbulence synchronization is expected in a rush environment partially dominated by incoherence. The weaker synchronization between chaotic systems, namely the phase synchronization occurs when the suitably well-defined phases collapse, while the amplitudes remain highly uncorrelated. Furthermore, in the case of chaotic systems having a broad range of time scales, the phases do not perfectly synchronize, but synchronization periods are interrupted by intermittent phase slips. The average duration between phase slips increases and becomes infinite as the coupling strength or driving frequency becomes

closer to the critical transition point of synchronization of self-sustained periodic oscillators. In the presence of noise, or of incoherence as in the case of the wall turbulence, the lengths of laminar segments whether in or outer synchrony are random. The noisy synchronization is commonly defined as stochastic synchronization, and the phase locking occurs for random periods of times and is interrupted by random phase slips[11,12,13]. The synchronization of the wall turbulence driven by coherent vortices advecting in the low buffer layer, if it occurs, should be classified in this last category.

Special techniques are necessary to detect the synchronization, which is generally hidden in phase synchronization of chaotic systems and in stochastic synchronization that is further difficult to depict. We apply the instantaneous amplitude phase concept to the scale decomposed turbulent quantities in the present investigation. The scale decomposition is obtained through wavelet analysis. The instantaneous phase concept is widely used in the theory of nonlinear oscillations and waves and in communication theory[14]. It has also been applied to the phase synchronization phenomena in coupled chaotic systems[15]. It is however not efficient without the scale decomposition in the synchronization analysis of the wall turbulence.

Dynamical systems approach of the wall turbulence is far being new[16], but we believe that the results presented in this paper are rather original for our community. Synchronization means existence of unstable periodic orbits. Besides its attractivity from a fundamental point of view, synchronization concept may be useful to develop new strategies of wall turbulence control in parallel with chaos control[17]. Thus, small time-dependent perturbations may be introduced in the system parameters to improve a desired response, such as drag reduction or mixing enhancement.

The paper is divided into four parts. The experiments we performed are described in the next session. The session 3 is devoted to detailed data analysis technique we used. The results are presented in the session 4.

2 Experiments

The ensemble of the measurements reported here have been realized in the low speed wind tunnel of LEGI. The boundary layer and momentum thickness at the test section were respectively $\delta = 34\,mm$ and $\theta = 3.4\,mm$. The Reynolds number based on the local momentum thickness is $Re_\theta = 913$, while the free stream velocity was $U_\infty = 4\,m/s$

3 Data analysis

The window average gradient scheme (WAG) was introduced by Antonia and Fulachier[19] and widely used in studies dealing with different flow configurations for example in Antonia et al.[20] and Krogstad and Antonia[21]. This scheme has been developed to detect the discontinuities in the fluctuating velocity signals and mainly been applied to wall bounded flows, although not exclusively. The continuous version of the WAG detection scheme is defined through a moving window of width $2T_w$ and the data is transformed into:

$$W(t,T_w) = \frac{1}{2T_w}\left(\int_t^{t+T_w} u(t)\,dt - \int_{t-T_w}^{t} u(t)\,dt\right) \qquad (1)$$

where $u(t)$ is the fluctuating turbulent velocity signal. It can be easily seen that, $W(t,T_w)$ is the output of a *linear* system whose transfer function $h_W(t)$ is defined by:

$$h_W(t) = \begin{cases} \dfrac{1}{2T_w} & T_w \le t < 0 \\ -\dfrac{1}{2T_w} & 0 \le t < T_w \end{cases} \qquad (2)$$

and $h_W(t) = 0$ otherwise. Therefore, $W(t,T_w) = u(t) \otimes h_W(t)$, where $\otimes$ stands for the convolution operator. Since the input-output relationships of a linear system are determined through the deterministic autocorrelation function defined as the convolution:

$$\rho_W(t) = h_W(t) \otimes h^* W(-t) \qquad (3)$$

where the superscript * indicates the complex conjugate.

The wavelet transform $\Omega(k,t)$ of the signal $u(t)$ is defined by:

$$\Omega(k,t) = \sqrt{k}\; u(t) \otimes g(-kt) \qquad (4)$$

where $g(t)$ is the mother wavelet. The wavelet transform is covariant under time translation and scale change. It conserves the energy of the signal and is invertible provided that the admissibility condition is satisfied.

The window averaged gradient scheme defined in (1) is per se a wavelet transform since its transfer function $h_W(t)$ is admissible. It is indeed closely related to the Haar transform which is the simplest wavelet used in multiresolution analysis.

Any signal, moreover the wavelet coefficients $\Omega(k,t)$ may be expressed as:

$$\Omega(k,t) = r(k,t)\cos\left[\int_0^t \omega_i(k,t)\right] \qquad (5)$$

where $r(k,t)$ stands for the instantaneous amplitude and $\omega_i(k,t)$ is the instantaneous angular frequency at scale k. This representation is not unique and different characterizations are possible, depending upon the choice of the dual processes. In the Rice canonical representation that is optimum in the sense of minimizing the average rate of the signal envelope, one has:

$$r^2(k,t) = \Omega^2(k,t) + \breve{\Omega}^2(k,t) \qquad (6)$$

by using the Hilbert transform $\breve{\Omega}$ of Ω, and:

$$\omega_i(k,t)=\frac{\Omega(k,t)\breve{\Omega}'(k,t)-\Omega'(k,t)\breve{\Omega}(k,t)}{r^2(k,t)} \quad (7)$$

where ' denotes the time derivative. The corresponding optimum carrier frequency, equals:

$$\omega_c(k)=\frac{\overline{r^2(k,t)\omega_i(k,t)}}{\overline{r^2}(k,t)} \quad (8)$$

with $\varphi(k,t)$ being the random phase at scale *k*.

4 Results

A snapshot of the instantaneous phase $\varphi\left(k^+,t^+\right)$ and amplitude $r^+\left(k^+,t^+\right)$ of the fluctuating streamwise velocity signal u' at $y^+=10$ is shown in Fig.1 for the wavelet scale parameter $k^+=0.24$ (corresponding to the wavelet window duration $T_W^+=26$). It is recalled that the wavelet scale parameter k^+ is defined as $k^+=\frac{2\pi}{T_W^+}$. The optimum angular carrier frequency is $\omega_c{}^+=0.07$ in Fig.1. It is seen that the instantaneous phase $\varphi(k,t)$ consists of line segments that are discontinuous at points B and D where random phase jumps occur. The phase increases first at A-B, remains constant during a large period C-D, jumps again and increases at D-F. The constancy of the phase indicates that the instantaneous frequency is roughly equal to the carrier frequency. The periods like C-D wherein $\omega_i\approx\omega_c$ coincide generally with large amplitudes $r^+\left(k^+,t^+\right)$. Strong ejection-sweeps transitions marking the arrival of coherent structures are, therefore, merely constant phase events. The time intervals as A-B wherein $\varphi\left(k^+,t^+\right)$ increases while $r^+\left(k^+,t^+\right)$ decreases are reminiscent of apparition of small scales. The slop of A-B is $\frac{d\varphi^+}{dt^+}=\frac{\omega_c{}^+}{3}$ indicating that $\omega_i(k,t)$ is jumped by a factor 4/3. The jumps in frequency with the *same* fraction of $\omega_c{}^+$ are often and repetitively observed. The epochs as E-F, wherein both the instantaneous phase and the amplitude increase from small values, are presumably related to the arrival of smaller scale active structures. Note finally that, the duration of the segments is about 100-200 wall units that is close to the ejection (bursting) period in the low buffer layer [6,7].

The occurrence of these long periods is particularly interesting. They refer to the set-up of stochastic synchronization, and appearance of "laminar" periods[8] wherein the instantaneous frequency locks to the mean carrier frequency. The locking frequency corresponding to Fig. 1 is $f_c^+=\frac{\omega_c^+}{2\pi}=0.011$ which is precisely the median ejection frequency at $y^+\approx 15$ where the production reaches its maximum[7]. The physical interpretation of the occurrence of constant phase zones is related to the phase synchronization between the wall turbulent quantities and the forcing imposed by the coherent vortices generated and convecting near the wall. For phase synchronization of coupled chaotic oscillators with type-I intermittency, as it will be discussed in detail in the fallowing, a very large constant phase locked zone is fallowed by a very short turbulent stage (the turbulent stage here refers to periods wherein the signal is chaotic according to the terminology used in chaos synchronization). The difference here, is that, not only the duration of phase locked zones is random, but also that the phase *smoothly* fluctuates before sharp increases or phase jumps. Furthermore, zones like A-*B* wherein the phases increase do not exist in the case of coupled chaotic oscillators, that are subject to quiescent periods fallowed by rapid phase slips. This behaviour is due to the stochastic nature of the turbulence that is under the effect of incoherence. High frequency phase fluctuations superimposed on the low-pass segments are for example seen in the bottom of Fig.1. Their time scale t_s^+ is of the order of T_W^+ in this particular case. The high frequency components in $\varphi(k,t)$ affect only slightly the integral $\int_0^{t_D}\omega_i(k,t)\,dt=\omega_c(k)t_D+\int_0^{t_D}d\varphi(k,t)\,dt$ as long as t_S is small compared to the time scale t_D of the low-pass components.

The smooth temporal variations of the local amplitudes and phase synchronization of intermittent oscillations observed in Fig. 1 and 2 points at the existence of intermittency of some type where a large quiescent period is changed by very short duration jumps, until the next *laminar* stage. In the case of coupled chaotic oscillators, the phase synchronization coincides with a saddle-mode bifurcation and the intermittency just outside the synchronization zone is characterized by a type-I intermittency[8, 25,26]. Frequency synchronization is a matter of adjusting time-scales by interaction and can be established when the system is shifting among different time-scales and while the chaotic trajectories access to different unstable periodic orbits. In the case of perfect phase synchronization the average duration $\overline{T}_l$ of the phase locking regions separated by successive phase slips scales as:

$$\overline{T}_l\propto\left|C-C_{ps}\right|^{-\gamma} \quad (9)$$

where C is either the coupling strength or the frequency (wave number) of the driving signal. The exponent $\gamma>0$ is $\gamma=1$ in the case of on-off intermittency, and $\gamma=\frac{1}{2}$ for the type I intermittency. The parameter C_{ps} is the critical value of the phase

synchronization. Thus, infinitely long time periods of constant phase are expected in perfect synchronization as the driving parameter C becomes close to the critical C_{ps}. Such super long periods have for example been reported in chaotic Rössler oscillator driven by external forcing[26] . The type-I intermittency is connected to the saddle-node bifurcation whose universal form is $\frac{dx}{dt} = \left(C - C_{ps}\right) + x^2$. The time T_l for the system to move from $x = 0$ to $x \to \infty$ reads for:

$$T_l \propto \int_0^{\infty} \frac{dx}{\left(C - C_{ps}\right) + x^2} = \frac{\pi}{2}\left|C - C_{ps}\right|^{-1/2} \qquad (10)$$

where it is clearly seen that $\gamma = \frac{1}{2}$. In stochastic systems with incoherent turbulence (IT), it is impossible to observe perfect synchronization, similarly to noisy non-identical chaotic systems, The constant phase zones, interrupted by IT induced phase slips, are of finite length. The identification of phase synchronization in such systems is performed by computing the phase difference $\Delta\varphi$ that represents a pronounced peak near $\Delta\varphi = 0$ (Boccaletti et al.,[8], p. 61). However, according to Freund et al.[22] the identification of synchronization in the presence of noise is possible by quantifying the average duration $\bar{T}_l$ of locking epochs. Fig. 6 shows the distribution of relative phase constant zones occupancy $\vartheta = \frac{\bar{T}_l}{T_{total}}$ versus k^+. It is seen that ϑ goes through a well defined maximum at $k^{*+} = 0.25$ and $k^{*+} = 0.20$ for respectively u' at $y^+ = 10$ and τ', and decreases for larger and smaller wavelengths. This behavior points at some kind of intermittency. The maximum of ϑ is roughly 0.4 for τ' and slightly smaller for u'. Fig. 7 shows $\ln\vartheta$ versus $\ln\left|k^+ - k^{*+}\right|$. It is clearly seen that the type I intermittency with $\vartheta \propto \left|k^+ - k^{*+}\right|^{-1/2}$ holds reasonably well for $\left|k^+ - k^{*+}\right| \geq 0.14$. The lines with $-\frac{1}{2}$ slopes shown in Fig. 7 have been obtained through a regression analysis resulting in regression coefficients equal to 0.97. The deviation from the type I intermittency behavior takes place near the coupling wavelength $k \approx k^*$. This is expected since $\bar{T}_l$ should go to infinity at $k = k^*$ in perfect synchronization which is incompatible with the stochastic synchronization that is under the effect of incoherent turbulence.

Synchronization points at unstable periodic orbits (UPO) in chaotic systems. The spatiotemporal coherence in wall turbulence should presumably be given in one or more unstable periodic orbit embedded in turbulent attractors. The UPO's have recently been identified in Couette turbulence by Kawahara et al[27]. The periodic orbit they identified is of saddle nature, which is in agreement with the I-type intermittency observed here. The period of the UPO's they identified is $T_{UPO}{}^+ = 188$. A directly similar investigation does not exist in the case of fully developed turbulent channel flow. It is furthermore difficult to determine the period of the UPO's from the analysis conducted here. An estimation can however be given by using the carrier frequency at the coupling wavelength $k = k^*$. Curiously, both the fluctuating wall shear stress and the instantaneous velocity at $y^+ = 10$ gives sensibly $T_{UPO}{}^+ = \frac{2\pi}{\omega_c^+} = 90$ at $k = k^*$, which is nothing but once more the median ejection period in the low buffer layer.

5 Conclusion

A scale-instantaneous phase/amplitude representation of the near wall turbulence is introduced. The Rice representation is applied to the wavelet coefficients of the fluctuating wall shear stress and longitudinal velocity in the law buffer layer. The analytic signal concept causes an automatic separation of different time scales. This is due to the property of the Hilbert transformation to freeze slow variables. This, combined with the wavelet transform allows the analysis of separate scales and sorts out the hidden phase synchronization. Long quiescent periods of about 100 wall units length wherein the instantaneous phase is smoothly oscillating around constant values are noticed near the critical scale parameter. The constant phase zones are interrupted by rapid phase jumps. A parallelism is constructed between these behaviors and the stochastic synchronization of chaotic systems that are under the effect of noise, or incoherence as is the case of the near wall turbulence. The stochastic synchronization is caused by convecting coherent vortical structures near the wall. The detailed analysis of the data revealed the existence of type-I intermittency connected to the saddle-node bifurcation of the locking periods. The period of the unstable periodic orbit embedded in the turbulent attractor near the wall collapses well with that of the regeneration cycle of the coherent structures.

The occurrence of long quiescent periods of constant phases of the wavelet coefficients is interesting and may be used in some control strategies. The phase jumps in particular are unambiguously well defined near the critical wavelet scale parameter. The long time periods between the jumps annunciate the arrival of active structures. A gain in effectiveness may presumably be achieved if the decision and action stages of active control schemes coincide with these periods.

References

1. S.J. Kline, W.C. Reynolds, F.A. Schraub, P.W. Runstadler "The structure of turbulent boundary layer," J. Fluid Mech., **30**, 741, (1967).
2. R.A. Antonia "Conditional sampling in turbulence measurements" Ann. Rev. Fluid Mech., **13**, 131, (1981).
3. D.G. Bogard, W.G. Tiederman "Burst detection with single-point measurements" J. Fluid Mech, **162**, 389, (1986).
4. S.K. Robinson "Coherent motions in the turbulent boundary layer" Ann. Rev. Fluid Mech., **23**, 601, (1991).
5. J. Jeong, F. Hussain " On the identification of a vortex" J. Fluid Mech., **285**, 69, (1995).
6. S. Tardu "Characteristics of Single and Clusters of Bursting Events in the Inner Region of a Turbulent Channel Flow; Part 1: Shear Layer Events" Exp. Fluids, **20**, 112, (1995).
7. S. Tardu "Characteristics of Single and Clusters of Bursting Events in the Inner Region of a Turbulent Channel Flow; Part 2: Level Crossing Events" Exp. in Fluids, **33**, 640, (2002).
8. S. Boccaletti, J. Kurths, G. Osipov, D.L. Valladeres, C.S. Zhou, "The synchronization of chaotic systems" Phys. Rep., **366**, 1, (2002).
9. A.S. Pikovsky, M.G. Rosenblum, J. Kurths, "Synchronization. A Universal Concept in Nonlinear Sciences" Cambridge University Press, Cambridge (2001).
10. J. Kurths, S. Boccaletti, C. Grebogi, Y.C. Lai "Introduction: Control and synchronization in chaotic dynamical systems" Focus Issue: Control and synchronization in chaotic dynamical systems, Chaos, **13**,126, (2003).
11. J. Freund, A. Neiman, L. Schiemansky-Geier "Analytic description of noise induced synchronization" Europhysics Letters, **50**, 8, (2000).
12. L. Callenbach, P. Hanggi, S.J. Linz, J.A. Freund, L. Schiemansky-Geier "Oscillatory systems driven by noise: Frequency and phase synchronization" Phys. Rev. E, **65**, 051110, (2002).
13. A. Neiman, A. Silchenko, V. Anishchenko, L. Schiemansky-Geier "Stochastic resonance: noise enhanced phase coherence" Phys. Rev. E, **58**, 7118 (1998).
14. Middletown D. "An Introduction to Statistical Communication Theory "McGraw-Hill, New York, (1960).
15. M.G. Rosenblum., A.S. Pikovsky, J. Kurths, "Phase synchronization of chaotic oscillators" Phys. Rev. Lett., **76**, 1804, (1996).
16. P. Holmes, J.L. Lumley, G. Berkooz, Turbulence, Coherent Structures, Dynamical Systems and Symmetry, Cambridge Un. Press, Cambridge, (1996).
17. S. Boccaletti, C. Grebogi, Y.C. Lai, H. Mancini, D. Maza," The control of chaos: theory and applications," Phys. Rep., **329**, 103, (2000).
18. S. Tardu "Active control of near-wall turbulence" J. Fluid Mech.,**439**, 217, (2001).
19. R.A. Antonia, L. Fulachier L., 1989 "Topology of a turbulent boundary with and without wall suction" J. Fluid Mech., **198**, 429, (1989).
20. R.A. Antonia, D.K. Bisset , L.W.B. Browne "Effect of Reynolds number on the organized motion in a turbulent boundary layer" J. Fluid Mech. **213**, 267, (1990).
21. P.-A. Krogstad, R.A. Antonia "Structure of turbulent boundary layers on smooth and rough walls" J. Fluid Mech. , **277**, 1, (1994).
22. J.A. Freund, L. Schimansky-Geier, P. Hanggi "Frequency and phase synchronization in stochastic systems" Chaos, **13**, 225, (2003).
23. Z. Zheng, G. Hu, B. Hu "Phase slips and phase synchronization of coupled oscillators"
    Phy. Rev. Letters, **81**, 5318, (1998).
24. Silchenko, T. Kapitaniak, V. Anishchenko "Enhanced phase locking in a stochastic bistable system driven by a chaotic signal" Phys. Rev. E, **59**, 1593, (1999).
25. Y. Pameau, P. Manneville "Intermittent transition to turbulence in dissipative dynamical systems", Commun. Math. Phys., **74**, 189, (1980).
26. A. Pikovsky, M. Zaks, M. Rosenblum, G. Osipov, J. Kurths "Phase synchronization of chaotic oscillations in terms of periodic orbits" Chaos, **7**, 680,(1997).
27. G. Kawahara, S. Kida, L. van Veen, " Unstable periodic motion in turbulent flows," Nonlinear Processes in Geophysics, **13**, 499, (2006).

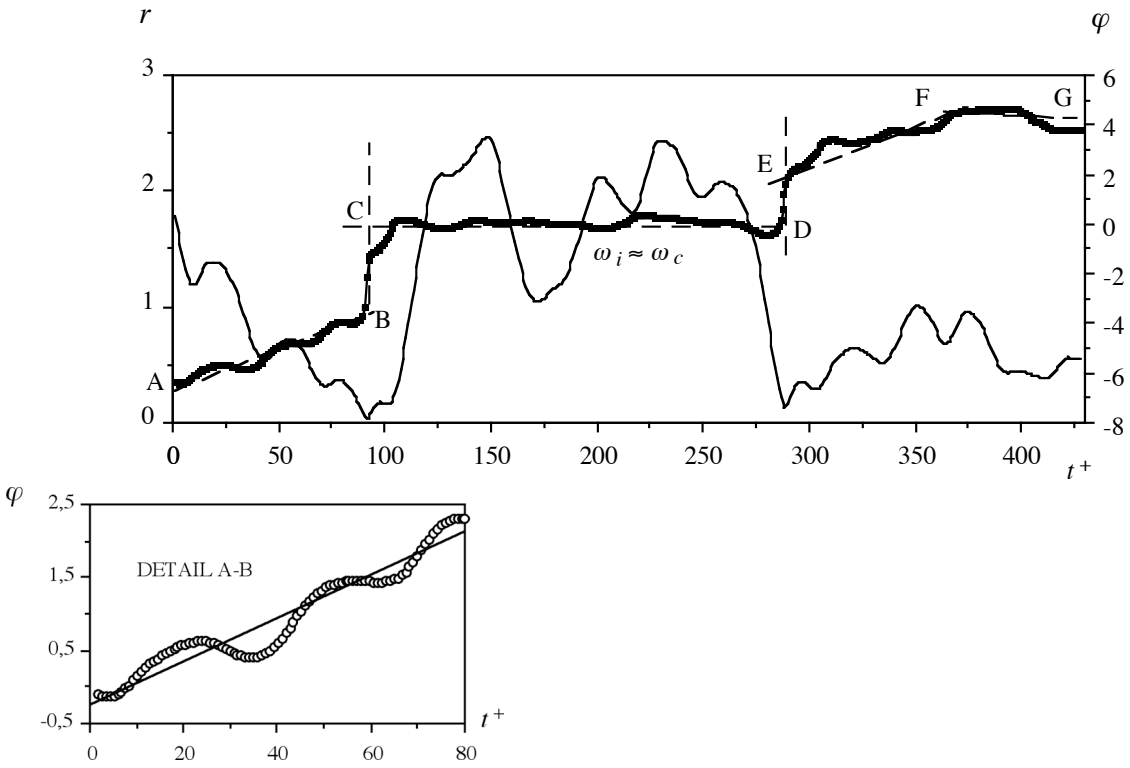

Figure 1 Samples of the instantaneous amplitude (continuous line) and phase (thick line) in radians of the WAG (Haar) wavelet coefficients of the fluctuating streamwise velocity at $y^+ = 10$ versus time .The scale parameter of the wavelet transform is $k^+ = 0.24$ in wall units.CD: Constant phase zone wherein the instantaneous frequency is equal to the carrier frequency. AB: The phase increases while the amplitude decreases: Apparition of small-scale structures. EF: The phase and amplitude increase simultaneously: Small-scale amplitude variations. DE: Phase jump. FG: Constant phase zone.

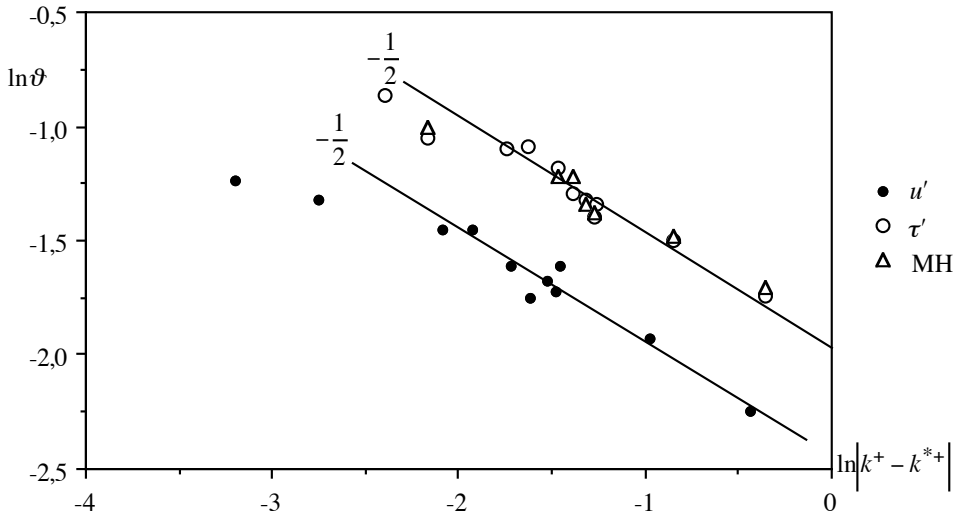

Figure 2 Relative occupancy versus wavelet scale parameter in log-log representation showing the existence of type-I intermittency. The triangles refer to the Mexican wavelet applied to the wall shear stress fluctuations.